PPPL-2285 192 1-15-85 JT (2) I-24513 PPPL-2285

UC20-A,F

(25)

PPPL--2285

DE86 005038

CONFINEMENT STUDIES OF NEUTRAL BEAM HEATED DISCHARGES IN TFTR

By

M. Murakami *et al*.

NOVEMBER 1985

PLASMA PHYSICS LABORATORY

PPL

PRINCETON UNIVERSITY
PRINCETON, NEW JERSEY

PREPARED FOR THE U.S. DEPARTMENT OF ENERGY,
UNDER CONTRACT DE-AC02-76-CHO-3073

CONFINEMENT STUDIES OF NEUTRAL BEAM HEATED DISCHARGES IN TFTR*

M. Murakami[a], V. Arunasalam, J.D. Bell[a], M.G. Bell, M. Bitter, W.R. Blanchard, F. Boody, N. Bretz, R. Budny, C.E. Bush[a], J.D. Callen[c], J.L. Cecchi, S. Cohen, R.J. Colchin[a], S.K. Combs[a], J. Coonrod, S.L. Davis, D. Dimock, H.F. Dylla, P.C. Efthimion, L.C. Emerson[a], A.C. England[a], H.P. Eubank, R. Fonck, E. Fredrickson, H.P. Furth, L.R. Grisham, S. von Goeler, R.J. Goldston, B. Grek, R. Groebner[d], R.J. Hawryluk, H. Hendel[e], K.W. Hill, D.L. Hillis[a], W. Heidbrink, R. Hulse, D. Johnson, L.C. Johnson, R. Kaita, R. Kamperschroer, S.M. Kaye, S. Kilpatrick, H. Kugel, P.H. LaMarche, R. Little, C.H. Ma[a], D. Manos, D. Mansfield, M. McCarthy, R.T. McCann, D.C. McCune, K. McGuire, D.M. Meade, S.S. Medley, S.L. Milora[a], D.R. Mikkelsen, D. Mueller, E. Nieschmidt[f], D.K. Owens, V.K. Pare[a], H. Park, B. Prichard, A. Ramsey, D.A. Rasmussen[a], M.H. Redi, A.L. Roquemore, P.H. Rutherford, N.R. Sauthoff, J. Schivell, G.L. Schmidt, S.D. Scott, S. Sesnic, M. Shimada[g], J.E. Simpkins[a], J. Sinnis, F. Stauffer[b], J. Strachan, B. Stratton. G.D. Tait, G. Taylor, C.E. Thomas[a], H.H. Towner M. Ulrickson, R. Wieland, J.B. Wilgen[a], M. Williams, K-L. Wong, S. Yoshikawa, K.M. Young, M.C. Zarnstorff, S. Zweben

Plasma Physics Laboratory, Princeton University
P.O. Box 451, Princeton, NJ 08544

[a]Permanent address: Oak Ridge National Laboratory, Oak Ridge, TN
[b]Permanent address: University of Maryland, College Park, MD
[c]Permanent address: University of Wisconsin, Madison, WI
[d]Permanent address: G.A. Technologies, Inc., San Diego, CA
[e]Permanent address: RCA David Sarnoff Research Center, Princeton, NJ
[f]Permanent address: EG&G, Idaho
[g]Permanent address: Japan Atomic Energy Research Institute, Japan

ABSTRACT

The TFTR tokamak has reached its original machine design specifications (I_p = 2.5 MA and B_T = 5.2T). Recently, the D° neutral beam heating power has been increased to 6.3 MW. By operating at low plasma current (I_p = 0.8 MA) and low density ($\bar{n}_e \approx 1 \times 10^{19} m^{-3}$), high ion temperatures (9 ± 2 keV) and rotation speeds (7×10^5 m/s) have been achieved during injection. At the opposite extreme, pellet injection into high current plasmas has been used to increase the line-average density to $8 \times 10^{19} m^{-3}$ and the central density to $1.6 \times 10^{20} m^{-3}$. This wide range of operating conditions has enabled us to conduct scaling studies of the global energy confinement time in both ohmically and beam heated discharges as well as more detailed transport studies of the profile dependence. In ohmic discharges, the energy confinement time is observed to scale linearly with density only up to $\bar{n}_e \sim 4.5 \times 10^{19} m^{-3}$ and then to increase more gradually, achieving a maximum value of ~ 0.45 s. In beam heated discharges, the energy confinement time is observed to decrease with beam power and to increase with plasma current. With P_b = 5.6 MW, $\bar{n}_e = 4.7 \times 10^{19} m^{-3}$, I_p = 2.2 MA and B_T = 4.7T, the gross energy confinement time is 0.22 s and $T_i(0)$ = 4.8 keV. Despite shallow penetration of D° beams (at the beam energy $\lesssim$ 80 keV with low species yield), $\tau_E(a)$ values are as large as those for H° injection, but central confinement times are substantially greater. This is a consequence of the insensitivity of the temperature and safety factor profile shapes to the heating profile. The radial variation of τ_E is even more pronounced with D° injection into high density pellet-injected plasmas.

KEYWORDS

Tokamaks, TFTR, Confinement, Neutral Beam Injection, Ohmic Heating, Scaling

*Presented at the 12th European Conference on Controlled Fusion and Plasma Physics, Budapest, Hungary, September 1985 (Invited talk). The proceedings are to be published in Plasma Physics and Controlled Fusion.

INTRODUCTION

Since the last IAEA conference (Efthimion and co-workers, 1985; Eubank and co-workers, 1985) the operating range of the TFTR tokamak has increased substantially with operation of the toroidal field, B_T, and plasma current, I_p up to the full design values of 5.2T (at major radius R = 2.48 m) and 2.5 MA. The total D^o neutral beam power has been increased up to 6.3 MW with the beam energy up to 90 keV. Both ohmic and neutral beam experiments have utilized the recently installed ORNL repeating pneumatic pellet injector (Combs and co-workers, 1985). In addition, an energetic ion regime, which is achieved by high power neutral beam injection into low density discharges, has been explored. Table 1 lists parameters of typical discharges in the different modes of operation.

TABLE 1 Parameters of Discharges in Various Modes of Operation

(R = 2.58m, a = 0.82m)

		Standard OH	Pellet OH	Standard NB	Pellet NB	Energetic Ion	Maximum (Minimum)
Shot		14618	13640	14734	14773	14281	--
I_p	[MA]	2.2	1.4	2.2	2.2	0.7	2.5
B_T	[T]	4.7	3.9	4.7	4.7	3.9	5.2
q_a		2.8	3.5	2.8	2.8	7.5	8 (2.3)
P_{inj}	[MW]	0	0	5.6	5.7	4.6	6.3
$\bar{n}_e$	$[10^{19}m^{-3}]$	4.8	7	4.7	7.0	1.0	7
$n_e(0)$	$[10^{19}m^{-3}]$	6.1	16	6.2	10.2	2.0	16
$T_e(0)$	[keV]	2.5	1.3	4.9	2.7	3.7	5
$T_i(0)$	[keV]	2.3	1.3	4.8	2.6	8.3±1.5	9±2
$\tau_E(a)$	[s]	0.44	0.45	0.22	0.22	~0.10	0.45

As a result of the extension in parameters, improved cleanliness, and the performance of the pellet injector, significant progress has been made in increasing the line-average electron density, $\bar{n}_e$, and the gross energy confinement time, $\tau_E(a)$. Neutral beam injection has been used to heat the plasma in both the "standard" regime at high density and high current as well as in the "energetic ion" regime at low density and current. The extended operating range has enabled us not only to explore the parametric dependence of the confinement time and heating efficiency, but also to study the role of "profile consistency" in establishing the profiles of electron temperature and safety factor, q(r). Even when a strongly non-central heating profile was applied, the temperature and pressure profile shapes were observed to be altered only weakly and no significant change was observed in the gross energy confinement, implying a relatively long energy confinement time in the core region.

This paper reviews the present status of confinement studies in TFTR. Following a brief description of the characteristics of ohmically heated plasmas, recent neutral beam heating and confinement results in the standard regime will be described. Afterwards, the results in the energetic ion regime will be summarized.

CONFINEMENT OF OHMICALLY HEATED PLASMAS

In the present extended operational range, ohmic-heating confinement studies have concentrated on exploring the range of applicability of the scaling law established previously, $\tau_E(a) \propto \bar{n}_e q_a R^2 a$ (Hawryluk and co-workers, 1984; Efthimion and co-workers, 1984) where $\bar{n}_e$ is the line-average density, and q_a is the cylindrical limiter safety factor. Figure 1 shows results of these studies. The extended operational space ranges to a minimum of $q_a \sim 2.4$, and a maximum density of $\bar{n}_e \sim 5.3 \times 10^{19} m^{-3}$ with D_2 gas puffing and $8 \times 10^{19} m^{-3}$ with either D_2 pellet injection or He gas puffing (corresponding to values of the parameter $\bar{n}_e(10^{19}m^{-3})\ R(m)/B_T\ (T)$ of 3.3 and 5.6 respectively).

The main impurity species in the TFTR plasma are carbon (the material of the outer moveable limiter) and oxygen. At low densities ($\bar{n}_e \approx 1 \times 10^{19} m^{-3}$), substantial contributions to Z_{eff} from nickel and titanium are observed, which decrease rapidly with increasing density. As the density limit is approached, oxygen line radiation increases and a poloidally asymmetric radiation feature, MARFE (Lipschultz and co-workers, 1984), appears on the inner major-radius periphery of the plasma. The initial application of chromium gettering prior to a run was effective in reducing the oxygen radiation, in increasing the density limit by 20% and in reducing Z_{eff} (from visible bremsstrahlung) to 1.4 at $\bar{n}_e = 4.7 \times 10^{19} m^{-3}$. The reduction in Z_{eff} and the radiated power fraction, P_{rad}/P_{OH}, to $\lesssim$ 40% from the levels previously reported (Hawryluk and co-workers, 1984; Efthimion and co-workers, 1984) is also strongly correlated with an uninterrupted high-power operating period of ≈ 2400 discharges.

The analysis of the energy confinement time was performed by using the time-independent snapshot radial-profile analysis code (SNAP). The largest value of $\tau_E(a)$ with D_2 puffing was 0.44 s at $\bar{n}_e = 4.8 \times 10^{19} m^{-3}$, which is roughly consistent with the scaling $\tau_E \propto \bar{n}_e q_a$. In He plasmas, $\tau_E(a)$ was observed not to scale linearly with $\bar{n}_e$ as the density was increased to $\bar{n}_e = 8 \times 10^{19} m^{-3}$. In high-density He plasmas, the dependence of τ_E on q_a was weaker than in D plasmas. Transport analysis of the high density He plasmas using TiXXI K_α Doppler broadening measurements of the ion temperature indicates that the roll-over in τ_E with density is due mainly to electron transport. A neoclassical multiplier necessary to explain the roll-over by ion transport alone gives rise to the difference between $T_e(0)$ and $T_i(0)$ substantially greater than the measured difference, including the experimental errors.

The initial ohmically heated pellet injection experiments have used two different pellet sizes (Schmidt and co-workers, 1985). A single 4 mm D_2 pellet raised $n_e(0)$ to $1.6 \times 10^{20} m^{-3}$, resulting in a substantially peaked density profile ($n_e(0)/\bar{n}_e = 2.0$, as opposed to ~ 1.4 with gas puffing). More extensive experiments have been made with multiple (up to 5) 2.7 mm pellets injected into a single discharge. Pellet injection has extended the $\bar{n}_e$ range to $8 \times 10^{19} m^{-3}$ in deuterium discharges, and has resulted in $n_e(0)\tau_E(a)$ of $7 \times 10^{19} m^{-3}$ s with $T_e(0)$ [$\approx T_i(0)$] of 1.3 keV. The value of $\tau_E(a)$ of 0.45 s is comparable to the largest value achieved with gas puffing.

GLOBAL CHARACTERISTICS OF BEAM-HEATED DISCHARGES

In this section, the discharge characteristics in the standard neutral beam heating regime and the dependence of the gross energy confinement time on neutral beam power, plasma current, and injection species will be described. D° beams were used to inject up to 6.3 MW into both D^+ and H^+ target plasmas while H° beams operating at reduced power ($\lesssim$ 4 MW) were injected into D^+ plasmas. Figure 2 compares the evolution of plasma current, surface voltage, and line-average electron density for an ohmic and a neutral beam heated deuterium discharge. These two discharges are among those in a power scan in which the beam heating power was varied systematically. The flat-top plasma current of 2.2 MA, with B_T = 4.7 T, R = 2.58 m, and a = 0.82 m corresponds to q_a of 2.8. In the neutral beam discharge, the total D° beam power (P_{inj}) was 5.6 MW from two co-tangential beamlines, each with three sources operating between 70 and 90 keV (78 keV average). The beam duration was 0.5 s. With injection $\bar{n}_e$ increased substantially (by ~ 50% at the highest power) consistent with the direct beam fueling rate (Murakami and co-workers, 1985). In order to obtain a constant

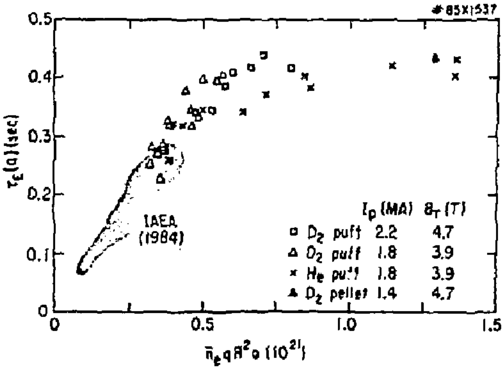

Fig. 1 Gross energy confinement versus $n_e q R^2 a$ for ohmically heated discharges with and without pellet injection.

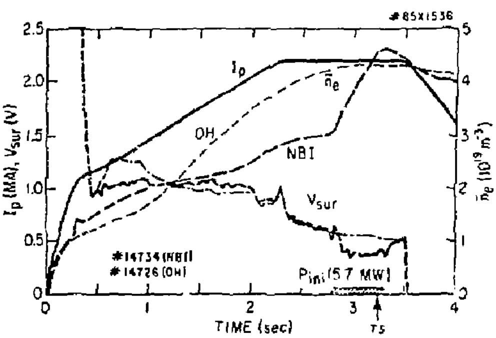

Fig. 2 Evolution of plasma parameters of discharges with ohmic heating (fine curves) and neutral beam injection (bold curves).

density just before the end of the beam pulse ($\bar{n}_e$ = 4.6 x $10^{19} m^{-3}$ at t = 3.25 s), the pre-injection density was adjusted. The surface voltage (V_{sur}) dropped from 1.1 V to 0.7 V during injection. The total radiated power (P_{rad}) increased with injection, but the fraction $P_{rad}/(P_{OH} + P_{inj})$ was reduced to ~ 20% from ~ 40% with ohmic heating alone. Impurity concentrations generally increased with increasing power, and both the visible bremsstrahlung measurement and the conductivity measurement (with the neoclassical correction) indicated that Z_{eff} increased from 2 to 3 as the neutral beam power increased up to 5.6 MW. Figure 3 shows variations of central electron temperature (from Thomson scattering) and central ion temperature (from TiXXI Doppler broadening) with absorbed beam power (P_{abs}). The sawtooth oscillation (or internal disruption) varied with respect to the Thomson scattering timing of 3.25 s at which detailed transport analyses were made. The bars shown indicate the variation of T_e during sawteeth (as measured from electron cyclotron emission) and the timing of the instantaneous Thomson scattering measurement within the sawtooth period. The Thomson scattering measurement for the discharge at the highest beam power happened to be made just before a large internal disruption, and the $T_e(0)$ value for this discharge is at the upper end of the bar. The Doppler broadening measurements of $T_i(0)$ have been corrected for radial emission profile effects ($\lesssim$ + 10%). In this regime, the difference between impurity and bulk ion temperature measurements is negligible. The line drawn in the figure corresponds to a central ion heating efficiency η_i ($\equiv \Delta T_i(0)\ \bar{n}_e/P_{abs}$) of 1.5 x 10^{19} keV m^{-3} MW^{-1}.

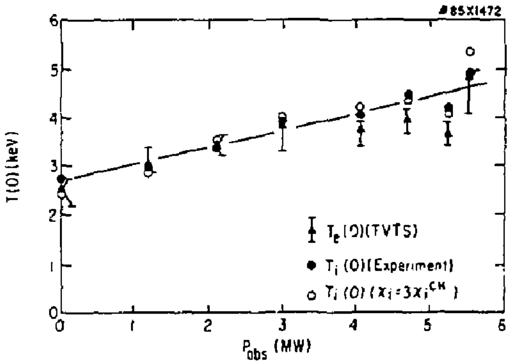

Fig. 3 Variations of central electron and ion temperature as a function of absorbed beam power. The central electron temperature from Thomson scattering is shown together with the amplitude of sawtooth oscillations of $T_e(0)$ from electron cyclotron emission measurements indicated by the bars. The experimental central ion temperature is compared with that predicted by a model based on $\chi_i = 3\chi_i^{CH}$.

Figure 4 shows the variation of the total stored energy ($W_p = W_e + W_i$) in the thermal ions (W_i) and electrons (W_e) with heating power (P_{heat}) for the 2.2 MA power scan and for 1.8 MA discharges utilizing either H° or D° injection. The changes in poloidal beta (β_p) due to beam injection as calculated by kinetic analysis agree (within ~ 10%) with diamagnetic measurements of $\Delta\beta_{p\perp}$ and equilibrium measurements of $\Delta\Lambda$. The heating power (P_{heat}) is defined as the sum of the ohmic (P_{OH}) and absorbed beam power (P_{abs}) less the calculated fast-ion charge-exchange loss (P_{cx}), which is typically $\lesssim$15% of P_{abs} in these experiments. The stored energy increases linearly with heating power to 1.3 MJ (total stored energy is 1.4 MJ, including the fast ion energy). However, the rate of increase of stored energy, dW_p/dP_{heat}, is appreciably less than the ohmic confinement time.

One possible explanation for the difference might have been that the beam power was not completely transferred to the plasma. However, the following observations eliminate this possibility. Nearly 100% (± 15%) power accountability has been demonstrated in various discharges by simultaneous measurements of radiative and charge exchange losses with bolometry and limiter power with an infrared photometry. This demonstrates that the beam power is being delivered to the torus. Furthermore, the power accountability is good even in neon-seeded discharges in which the fraction P_{rad}/P_{heat} approached one (Murakami and co-workers, 1985). Thus, the power transfer from the beams to the bulk plasma can not be seriously affected by either beam orbit losses or beam charge exchange which would not be measured by the perpendicular bolometer array. Tangential charge exchange spectra have also been examined to investigate possible enhanced beam ion losses. The spectra are reasonably consistent with classical expectations in D° injected discharges. Agreement was also observed during major-radius compression experiments in which the fast ions were accelerated from 82 to 150 keV (Wong and co-workers, 1985), consistent with classical expectation. These observations imply that the beam power is delivered to the plasma and thus the less-than-expected increase in stored energy is due to confinement degradation with the auxiliary heating.

The gross energy confinement time $\tau_E(a)$ ($\equiv W_p/P_{heat}$) for the data shown in Fig. 4 fits naturally to a form of $\alpha + \beta/P_{heat}$ where the "incremental" confinement time α = 0.10 s for 2.2 MA discharges. Within the scatter of the data, $\tau_E(a)$ can also be fit by a power law dependence of $P_{heat}^{-\gamma}$ where γ = 0.6. Figure 5 shows the variation of $\tau_E(a)$ with power, and shows a continuous deterioration with heating power. Also shown are empirical scaling laws derived by Goldston (1984) based on smaller tokamaks with neutral beam injection. [We express the term <nT> in Eq. (8) in Goldston (1984) in terms of (P_{heat} τ_E). The resulting form of Eq. (11) can be transformed to a quadratic equation for τ_E, and so solved. The τ_E calculated in this manner is $\gtrsim$ 10% higher in the transition region from ohmic to auxiliary heating than given by expressing <nT> in terms of (P_{heat} τ_E^{AUX}).]

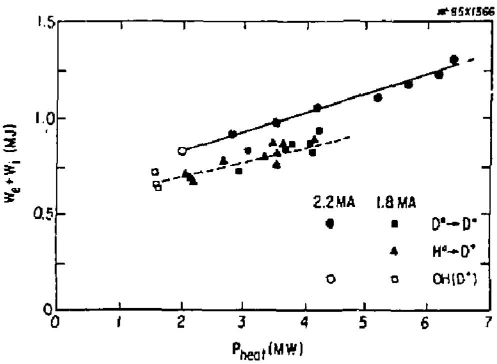

Fig. 4 Variation of the total stored thermal energy with heating power for the 2.2 MA power scan and 1.8 MA discharges utilizing both D° and H° injection.

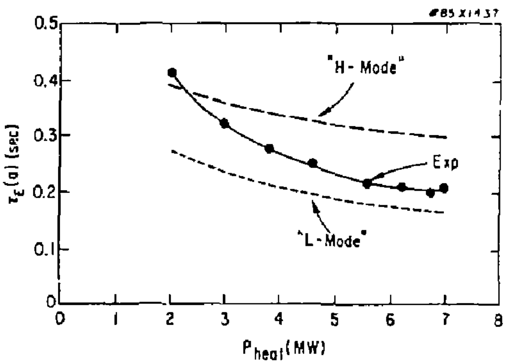

Fig. 5 Variation of the gross energy confinement time for the power scan and comparison with Goldston's (1984) L- and H-mode scaling predictions.

Figures 4, 6, and 7 show the dependences of $\tau_E(a)$ on injection species, density, and plasma current. Figure 4 demonstrates that there is no difference in $\tau_E(a)$ between H° and D° despite shallower penetration of D° beams compared to H° beams, as previously discussed (Murakami and co-workers, 1985). The insensitivity of $\tau_E(a)$ to beam penetration is also demonstrated in Fig. 6 which shows a weak dependence of $\tau_E(a)$ on the density in beam-heated discharges with and without pellet injection (Schmidt and co-workers, 1985). These points will be discussed in more detail below. Furthermore, Fig. 7 shows that $\tau_E(a)$ increases approximately linearly with I_p, as found in smaller tokamaks with injection. At the highest plasma current, $\tau_E(a)$ is somewhat larger than the Goldston L-mode scaling. The strong plasma current dependence is encouraging. Indeed, at I_p = 2.2 MA, a $\tau_E(a)$ value of 0.22 s has been achieved at $\bar{n}_e = 4.7 \times 10^{19}$ m^{-3} with $T_i(0)$ = 4.8 keV.

As we have discussed, confinement behavior of beam heated discharges are different from that of ohmically heated discharges. Conventionally, the energy transport in tokamaks has been described by a three region model: a core region where internal disruptions are important; a confinement region outside the core where a large pressure gradient is sustained; and an edge region dominated by a combination of atomic physics effects and rapid transport. This model will be used as a basis for discussing the behavior of the TFTR discharges. The transport in the confinement region will be discussed and then that in the core region. The role of the plasma edge will be discussed in relationship with our future work.

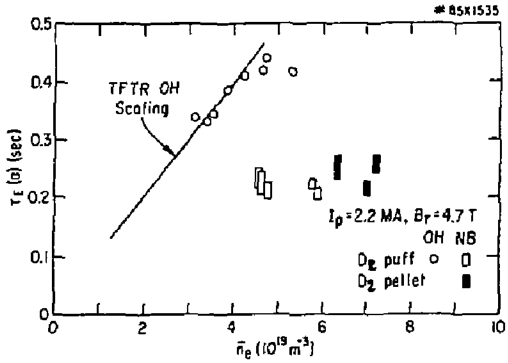

Fig. 6 Dependence of gross energy confinement on density for beam-heated discharges with and without pellet-fueling, as compared with that for ohmically-heated discharges.

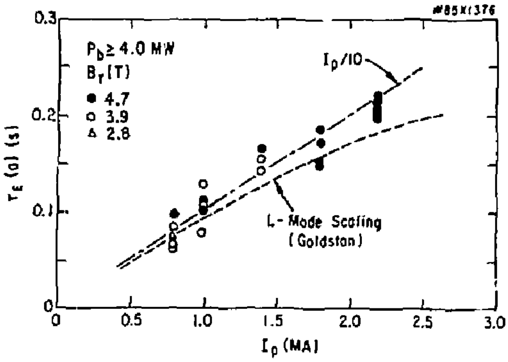

Fig. 7 Dependence of the gross energy confinement on plasma current.

ENERGY TRANSPORT IN THE CONFINEMENT REGION

The 2.2 MA power scan described in the previous section was used to study the variation of plasma transport with beam power. Both SNAP and the time-dependent transport analysis code TRANSP (Hawryluk, 1980; Goldston and co-workers, 1981) have been used. The radius of 2a/3 was chosen to represent the confinement region. In this analysis, χ_i was assumed to be equal to 3 χ_i^{CH} where χ_i^{CH} is the neoclassical ion thermal diffusivity (Chang and Hinton, 1982). Ion temperatures were calculated on the basis of the instantaneous Thomson scattering profile, and no attempt was made to include direct effects of sawteeth on the ion power balance. Figure 3 shows that the predicted ion temperature is in agreement with the experimental values, especially when the uncertainties in both $T_e(0)$ and $T_i(0)$ are taken into account. Classical beam power deposition and slowing-down calculations using a Fokker-Planck code (in SNAP) and a Monte-Carlo code (in TRANSP) show most (~ 4/5) of the beam power is transferred to the ions in the power scan experiments. However a substantial portion of the power to the ions (P_{bi}) is then coupled to the electrons through classical electron-ion collisions. In fact, about 80% of the total heating power is lost by the electron channel throughout the entire range of beam power. Since the electron stored energy within r = 2a/3 is only 40-50% larger than the ion energy, the electron energy confinement τ_{Ee} (2a/3) is substantially smaller than the ion confinement time τ_{Ei}(2a/3) and the total energy confinement is largely determined by the electron confinement, as shown in Fig. 8(a). Uncertainties in the ion heat conductivity multiplier of ± 50% would alter τ_{Ei} by 30% while τ_{Ee} and τ_E hardly change (< 5%).

As perhaps expected from the deterioration of τ_{Ee} with increasing beam power, the electron thermal diffusivity χ_e(2a/3) increases with increasing beam power, as shown in Fig. 8(b). The χ_e value further out (e.g., r = 0.8a) rises more decisively with beam power. However, in the core region, the χ_e value at r = 0.4a stays level or decreases with increasing P_{abs} as described below.

CONFINEMENT IN THE CORE REGION

The confinement characteristics of the core region are not only of great fundamental interest but also of importance for the performance of future ignition devices. The obvious phenomena in the central region are the sawtooth oscillations (internal disruptions), (McGuire and co-workers, 1985), which are believed, however, to play a minor role in the overall energy balance. Both the location of q = 1 surface and the electron temperature profile shape are observed to be functions of the limiter safety factor and not of the heating profile. One interesting consequence is that for non-central heating profiles the central confinement during injection can be appreciably longer than the gross energy confinement time.

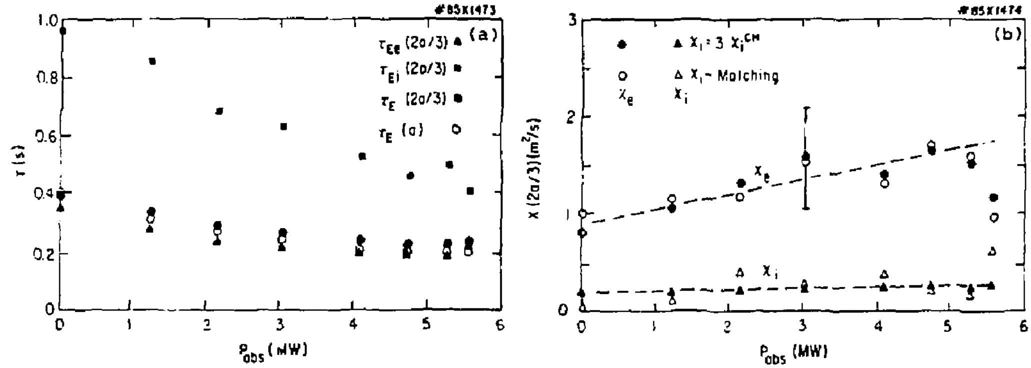

Fig. 8 Results of power balance analyses for the power scan: (a) the solid points show variations of the electron (τ_{Ee}), ion (τ_{Ei}) and total (τ_E) *energy confinement time, all evaluated at* $r = 2a/3$, *with absorbed* beam power. The open circles are the gross energy confinement time, $\tau_E(a)$; (b) the solid points show electron (χ_e) and ion (χ_i) thermal diffusivity as functions of beam absorbed power, assuming that $\chi_i = 3\ \chi_i^{CH}$. The open points are deduced ion thermal diffusivities required to *match* the measured $T_i(0)$.

Figures 9(a), (b) and (c) show the responses of $T_e(0)$, $T_i(0)$, and central rotation, $V_\phi(0)$, *to internal disruptions* in a $q_a = 3.6$ beam-heated discharge. Figure 9(d) compares two T_e profiles (from electron cyclotron emission) before and after an internal disruption. There is also a modest (< 5%) variation of $n_e(0)$ deduced from a 5-channel FIR interferometer. Based on these profiles, *the thermal energy within a radius, r, has been calculated,* as shown in Fig. 9(e). The change in the stored thermal energy as a result of the internal

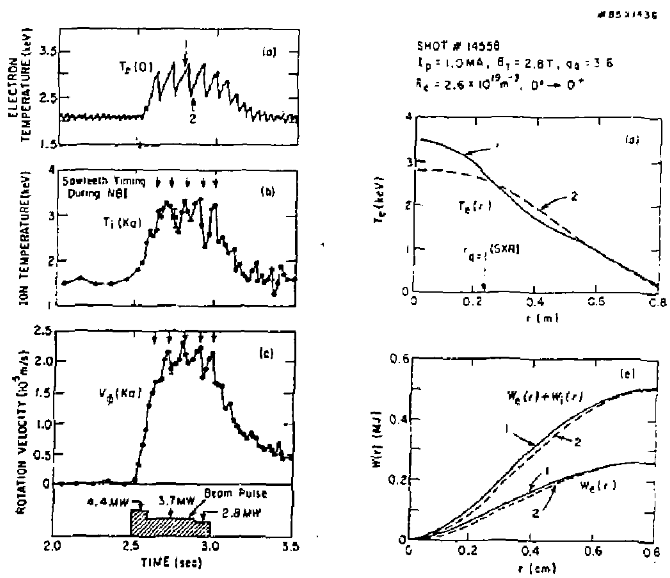

Fig. 9 Effects of sawtooth oscillations in a beam-heated discharge: (a) *the central electron temperature (from electron cyclotron emission measurements);* (b) *the uncorrected ion temperature (from TiKα); (c)* the central toroidal rotation velocity (from TiKα); (d) comparison of T_e profiles before and after the internal disruption at the times indicated in (a); and *(e) comparison of the* electron and ion stored energy before and after the internal disruption.

disruption is small. The neutron source rate, which is dominated by beam-target reactions does not show substantial reductions as a result of the internal disruption, indicating that there is no significant loss of beam ions. A confinement time associated with sawtooth oscillations, $\tau_E^{ST} = t_{st}T_e/\Delta T_e$ (where t_{st} is the sawtooth period), is of the order of 0.7 s: much longer than either the gross or electron energy confinement times. In the power scan experiment, τ_E^{ST} is also ~ 0.7 s, independent of beam power.

In addition, it has been observed in the TFTR ohmic heating studies that $T_e(r)$ profiles are determined by q_a (Taylor and co-workers, 1985). Similarly, in PDX neutral beam heating studies (Goldston, 1984; Kaye and co-workers, 1984) the ratio $\langle T_e\rangle/T_e(0)$, where $\langle T_e\rangle$ is the volume-average T_e, was observed to be a function of $1/q_a$, independent of beam power. Figure 10 shows the sawtooth-averaged $\langle T_e\rangle/T_e(0)$ as a function of $1/q_a$, and Fig. 11 illustrates the variation of the q = 1 radius (as determined by the soft X-ray imaging system) with $1/q_a$ for the same TFTR data set. That both $\langle T_e\rangle/T_e(0)$ and $r(q = 1)/a$ are uniquely determined by $1/q_a$ implies that there are natural profile shapes for $T_e(r)$ and $q(r)$ associated with the limiter safety factor. Coppi (1980), Perkins (1984), and others have discussed the significance of a constrained profile shape for anomalous transport. Recently, Furth (1985), and Furth and co-workers (1985) have discussed the constraints on current profile shape imposed by the resistive kink stability requirements and its ramifications.

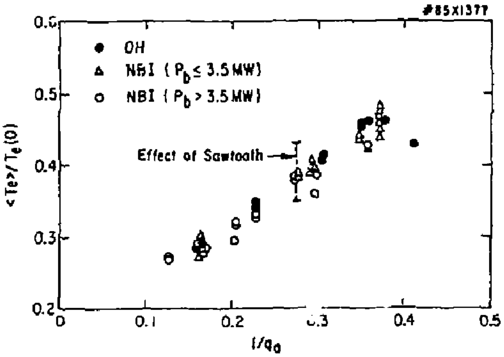

Fig. 10 Ratio of volume-average electron temperature to central electron temperature as a function of the inverse of the limiter safety factor. All data points are averaged over several sawtooth periods, except the data shown by a vertical line which is bounded by two values for the $T_e(r)$ profiles (shown in 9d) before and after the large internal disruption.

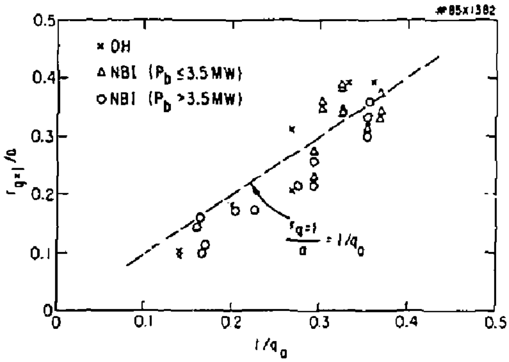

Fig. 11 Normalized q = 1 rational surface as a function of the inverse of the limiter safety factor.

It was found in TFTR (Murakami and co-workers 1985) that, despite shallow penetration of D° injection, $\tau_E(a)$ values are as large as those with more penetrating H° injection, and that the central core confinement is substantially greater with D° injection. Not only is the T_e profile shape indistinguishable between D° and H° injection, but the $T_e(0)$ and $T_i(0)$ values themselves are about equal to those with H° injection in TFTR. Similar results have been obtained in neutral beam heating experiments in ASDEX (Speth and co-workers, 1985). These observations are similar to the T-10 electron cyclotron heating results which showed that $\tau_E(a)$ remained roughly constant as the resonance layer was moved from r = 0 to r ~ 0.7a (Alikaev and co-workers, 1985). D° injection into high-density pellet-injected plasmas in TFTR (Schmidt and co-workers, 1985) have demonstrated the same phenomenon in even more striking form. Figure 12 shows the fraction (F_W) of the plasma stored energy within r = a/3 as a function of the fraction (F_p) of the heating power deposited within r = a/3. In ohmic discharges (shown by the hatched area including ~ 200 shots with a q_a range similar to the neutral beam case), F_W increases as F_p is raised by increasing q_a. With neutral beam injection, F_p can be changed in a much wider range. A change in F_p by a factor of 5 still leads to a range of F_W as narrow as the ohmic case, and the F_W variation is basically governed by q_a rather than by F_p. Since $F_W/F_p = \tau_E(a/3)/\tau_E(a)$, this indicates that the core confinement with poorly penetrating beams (in particular with pellet-fueled beam-heated plasmas) is substantially greater than the gross energy confinement.

Since the beam heating profile F_p is primarily governed by density, the central energy confinement tends to improve with increasing plasma density as shown in Fig. 13. In fact, within the presently available data, $\chi_e(a/3)$ is not much different from the INTOR type $\chi_e = 5 \times 10^{19}/n_e$. However, this conclusion should be taken with care, since the available $\bar{n}_e$ range for a given value of I_p is limited (as seen in Fig. 13) and analyses of data are incomplete at this time.

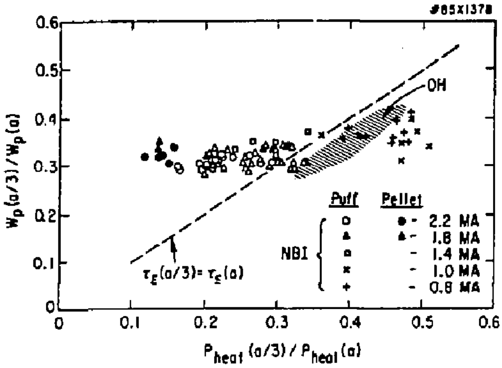

Fig. 12 Fractional total stored energy within r = a/3 versus fractional heating power deposited within r = a/3. The shaded areas are the areas occupied by a large number (~ 200) of ohmically heated discharges.

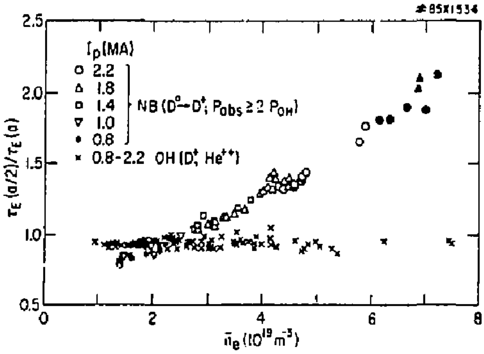

Fig. 13 Ratio of total energy confinement time at r = a/2 to gross energy confinement time as a function of density for both beam and ohmically-heated discharges. Closed circles and triangles show beam-heated discharges with pellet injection.

ENERGETIC ION REGIME

Operation of TFTR at low I_p (0.4–1.0 MA) and high beam power has allowed access to a very-low-density regime ($\bar{n}_e \sim 1 \times 10^{19}\ m^{-3}$) characterized by high ion temperature and high toroidal rotation velocity [Grove and Meade (1985)]. Figure 14 shows the time evolution of uncorrected ion temperature measurements (from TiXXI X-ray Doppler broadening and perpendicular passive hydrogen charge-exchange analysis) and of central electron temperature (from electron cyclotron emission measurements) for a typical discharge in this regime. Substantial corrections to the raw ion temperatures are calculated (Medley and co-workers, 1985). The dominant adjustment to the Doppler broadening measurement is the expected temperature difference between impurities and hydrogenic ions, which is maintained by preferential coupling of the beam power to impurity ions (Eubank and co-workers, 1978). The charge exchange analysis is corrected for opacity and for the high rotation velocity. The thermalized central hydrogenic ion temperature is calculated to be 8.3 ± 1.5 keV on the basis of both measurements. The ion heating rate calculated from this temperature is similar to that obtained in the standard neutral beam regime. The toroidal rotation velocity (as measured from Doppler shift of TiXXI K_α line radiation) observed in this discharge is 6.5×10^5 m/s, corresponding to a ratio of the rotation velocity to the deuteron thermal velocity ($V_{i,th} \equiv (T_i(0)/m_i)^{1/2}$) of ~ 1. The rotation velocity increases linearly with $P_{inj}/\bar{n}_e$ throughout the entire operating regime (with a tne only weak function of I_p), as shown in Fig. 15. Analysis of this discharge indicates that the beam ion density is almost as large as the background ion density and that the average central ion energy (~ 23 keV) is ~ 70% due to unthermalized beam ions. The high rotation velocity substantially complicates the energy transport analysis: direct beam heating is reduced, but additional viscous heating terms arise. The effort to include these effects in the analysis is in progress. Preliminary analysis shows that the ion power balance is dominated by convection and that $\tau_E(a)$ is of order 100 ms. Despite a relatively large population of beam ions in the plasma, behavior of ion heating, momentum confinement and global energy confinement are similar to those observed in the standard neutral beam regime.

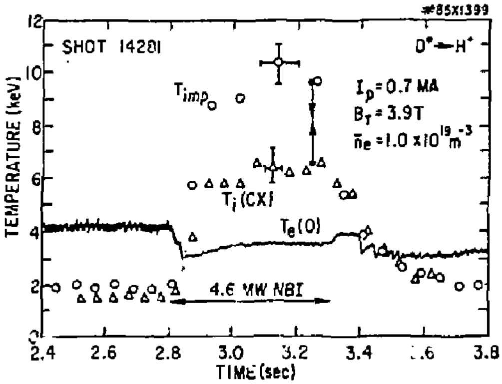

Fig. 14 Uncorrected ion temperature measurements based on Doppler broadening of TiKα lines (T_{imp}) and perpendicular charge-exchange spectra [T_i(cx)] in a *discharge in the energetic ion regime.* The correction to the measurements indicate a central ion temperature of 8.3 ± 1.5 keV, as shown by the arrows.

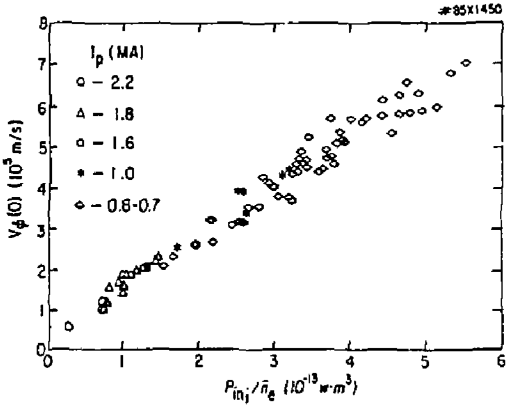

Fig. 15 Central toroidal rotation velocity as a function of the ratio of injected beam power to line-average *electron density.*

There are several additional interesting features of this new regime. (1) The surface voltage during injection decreases substantially to ~ 0.05V. The surface voltage at the end of the injection pulse decreases with increasing power and increases with plasma current. TRANSP analyses and BALDUR simulations, which do not include toroidal rotation, predict a neutral beam driven current of ~ 300 kA. (2) A relatively high neutron source strength (4 x 10^{14}/s) has been obtained in this regime.

This regime is of interest not only for its intriguing physics, but also for its relevance to the two-component mode of operation for which TFTR was designed. Future experiments will seek a better understanding and optimization of this regime.

CONCLUSIONS

Recent ohmic and neutral beam heating experiments have resulted in substantial improvements in plasma parameters. Ohmic discharges spanning a wide range of operating parameters clearly provide good target plasmas for neutral beam injection. With the recent installation of two additional neutral beamlines and provisions for higher voltage operation and for varying injection angle, confinement studies of higher power injection experiments will be focussed on further extending the plasma parameters and on obtaining a clearer understanding of the transport properties. The observation that the temperature profile is a weak function of heating profile suggests a couple of intriguing experimental implications (Furth, 1985). First, the properties of the edge region determine the local temperature there, and possibly therefore the overall stored energy and central temperature, since the shape of the overall temperature profile is relatively fixed. Hence better control of the plasma edge region may be crucial to attain improved gross energy confinement in high power beam injection experiments, as suggested by studies of various enhanced confinement modes. Second, since high density non-central heating profiles can result in favorable central confinement time, this regime could lend itself to the detection and study of alpha-particle effects in future DT experiments at modest overall Q.

ACKNOWLEDGEMENTS

It is a pleasure to acknowledge the very many engineers, computer programmers, and technicians whose dedicated efforts have enabled us to conduct these experiments. We are grateful to D. J. Grove and J. R. Thompson for advice and support. The work was supported by the US Department of Energy Contract No. DE-AC02-76-CHO3073. The ORNL participants were also supported by US Department of Energy Contract No. DE-AC05-84OR21400 with Martin Marietta Energy Systems, Inc.

REFERENCES

Alikaev, V.V. and co-workers (1985). Electron cyclotron heating and plasma confinement in the T-10 tokamak. In Plasma Phys. and Cont. Nucl. Fusion Research I IAEA, Vienna, 419.

Chang, C.S. and Hinton, F.L. (1982). Effect of finite aspect ratio on the neoclassical ion thermal conductivity in the banana regime. Phys. Fluids 25, 1443.

Combs, S.K. and co-workers (1985). Repeating pneumatic hydrogen pellet injector for plasma fueling. Rev. Sci. Instrum. 56, 1173.

Coppi, B. (1980). Nonclassical transport and the "principle of profile consistency." Comments Plasma Phys. Cont. Fusion 5, 261.

Efthimion, P.C. and co-workers (1984). Initial confinement studies of ohmically heated plasmas in the Tokamak Fusion Test Reactor. Phys. Rev. Lett. 52, 1492.

Efthimion, P.C. and co-workers (1985). Confinement studies of ohmically heated plasmas in TFTR. In Plasma Physics and Controlled Nuclear Fusion Research I IAEA, Vienna, 29.

Eubank, H.P. and co-workers (1979). PLT neutral beam heating results. In Plasma Physics and Controlled Nuclear Fusion Research I IAEA, Vienna, 167.

Eubank, H.P. and co-workers (1985). Neutral-beam heating in TFTR - projections and initial results. In Plasma Physics and Controlled Nuclear Fusion Research I IAEA, Vienna, 303.

Furth, H.P. and co-workers (1985). The q(0) < 1 regime of the tokamak. In Proc. 12th European Conf. on Cont. Fusion and Plasma Physics (Budapest, Hungary), Contr. papers II, 358.

Furth, H.P. (1985). Three novel tokamak plasma regimes in TFTR. Workshop on Basic Physical Processes of Toroidal Fusion Plasmas (Varenna, Italy), August 26-31, 1985 (to be published).

Goldston, R.J. and co-workers (1981). New techniques for calculating heat and particle source rates due to neutral beam injection in axisymmetric tokamaks. J. Comput. Phys. 43, 61.

Goldston, R.J. (1984). Energy confinement scaling in Tokamaks: Some implications of recent experiments with ohmic and strong auxiliary heating. Plasma Phys. and Contr. Fusion 26, 87.

Grove, D.J. and D.M. Meade (1985). Initial studies of confinement, adiabatic compression, and neutral-beam heating in TFTR. To be published in Nucl. Fusion.

Hawryluk, R.J. and co-workers (1984). Recent results from TFTR. In Proc. 4th Inter. Symp. on Heating in Toroidal Plasmas, Rome (Inter. School of Plasma Physics, Varenna) 1012.

Hawryluk, R.J. (1980). An empirical approach to tokamak transport. In Proc. of the Course in Physics Close to Thermonuclear Conditions (Varenna, Italy), Report EUR-FU-BRU/XII/476/80.

Kaye, S.M, and co-workers (1984). Studies of thermal energy confinement scaling in PDX plasmas: D^o+H^+ limiter discharges. Nucl. Fusion 24, 1303.

Lipschultz, B. and co-workers (1984). MARFE: an edge plasma phenomenon. Nucl. Fusion 24, 977.

McGuire, K. and co-workers (1985). Compound sawteeth and heat pulse propagation in TFTR. In Proc. 12th European Conf. on Controlled Fusion and Plasma Physics (Budapest, Hungary), Contr. papers I, 134.

Medley, S., and co-workers (1985). Ion behavior in TFTR during ohmic and neutral beam operation. In Proc. 12th European Conf. on Controlled Fusion and Plasma Physics (Budapest, Hungary), Contr. papers I, 343.

Murakami, M., and co-workers (1985). Confinement studies in TFTR. PPPL Report #2224 (June 1985); Proc. 6th Topical Meeting on the Technology of Fusion Energy (San Francisco, March 1985), Fusion Technology 8, part 2A, 657.

Perkins, F.W. (1984). Confinement scaling in tokamak: consequence of drift wave turbulence. In Proc. 4th Int. Symp. on Heating in Toroidal Plasmas, Rome (Int. School of Plasma Physics, Varenna) 977.

Schmidt, G.L., and co-workers (1985). Production of high density plasma by pellet injection in TFTR. In Proc. 12th European Conf. on Controlled Fusion and Plasma Physics (Budapest, Hungary), Contr. papers II, 674.

Speth, E., and co-workers (1985). The effect of neutral beam deposition on heating and confinement in ASDEX. In Proc. 12th European Conf. on Controlled Fusion and Plasma Physics (Budapest, Hungary), Contr. Papers II, 284.

Taylor, G., and co-workers (1985). Evolution of the electron temperature profile of ohmically heated plasmas in TFTR. PPPL Report #2221. (August 1985); submitted for publication to Nucl. Fusion.

Wong, K.L., and co-workers (1985). Acceleration of beam ions during major radius compression in TFTR. PPPL Report #2247. (September 1985); submitted to Phys. Rev. Lett.

EXTERNAL DISTRIBUTION IN ADDITION TO UC-20

Plasma Res Lab, Austra Nat'l Univ, AUSTRALIA
Dr. Frank J. Paoloni, Univ of Wollongong, AUSTRALIA
Prof. I.R. Jones, Flinders Univ., AUSTRALIA
Prof. M.H. Brennan, Univ Sydney, AUSTRALIA
Prof. F. Cap, Inst Theo Phys, AUSTRIA
Prof. Frank Verheest, Inst theoretische, BELGIUM
Dr. D. Palumbo, Dg XII Fusion Prog, BELGIUM
Ecole Royale Militaire, Lab de Phys Plasmas, BELGIUM
Dr. P.H. Sakanaka, Univ Estadual, BRAZIL
Dr. C.R. James, Univ of Alberta, CANADA
Prof. J. Teichmann, Univ of Montreal, CANADA
Dr. H.M. Skarsgard, Univ of Saskatchewan, CANADA
Prof. S.R. Sreenivasan, University of Calgary, CANADA
Prof. Tudor W. Johnston, INRS-Energie, CANADA
Dr. Hannes Barnard, Univ British Columbia, CANADA
Dr. M.P. Bachynski, MPB Technologies, Inc., CANADA
Chalk River, Nucl Lab, CANADA
Zhengwu Li, SW Inst Physics, CHINA
Library, Tsing Hua University, CHINA
Librarian, Institute of Physics, CHINA
Inst Plasma Phys, Academia Sinica, CHINA
Dr. Peter Lukac, Komenskeho Univ, CZECHOSLOVAKIA
The Librarian, Culham Laboratory, ENGLAND
Prof. Schatzman, Observatoire de Nice, FRANCE
J. Radet, CEN-BP6, FRANCE
AM Dupas Library, AM Dupas Library, FRANCE
Dr. Tom Mual, Academy Bibliographic, HONG KONG
Preprint Library, Cent Res Inst Phys, HUNGARY
Dr. R.K. Chhajlani, Vikram Univ. INDIA
Dr. B. Dasgupta, Saha Inst, INDIA
Dr. P. Kaw, Physical Research Lab, INDIA
Dr. Phillip Rosenau, Israel Inst Tech, ISRAEL
Prof. S. Cuperman, Tel Aviv University, ISRAEL
Prof. G. Rostagni, Univ Di Padova, ITALY
Librarian, Int'l Ctr Theo Phys, ITALY
Miss Clelia De Palo, Assoc EURATOM-ENEA, ITALY
Biblioteca, del CNR EURATOM, ITALY
Dr. H. Yamato, Toshiba Res & Dev, JAPAN
Direc. Dept. Lg. Tokamak Dev. JAERI, JAPAN
Prof. Nobuyuki Inoue, University of Tokyo, JAPAN
Research Info Center, Nagoya University, JAPAN
Prof. Kyoji Nishikawa, Univ of Hiroshima, JAPAN
Prof. Sigeru Mori, JAERI, JAPAN
Prof. S. Tanaka, Kyoto University, JAPAN
Library, Kyoto University, JAPAN
Prof. Ichiro Kawakami, Nihon Univ, JAPAN
Prof. Satoshi Itoh, Kyushu University, JAPAN
Dr. D.I. Choi, Adv. Inst Sci & Tech, KOREA
Tech Info Division, KAERI, KOREA
Bibliotheek, Fom-Inst Voor Plasma, NETHERLANDS
Prof. B.S. Liley, University of Waikato, NEW ZEALAND
Prof. J.A.C. Cabral, Inst Superior Tecn, PORTUGAL
Dr. Octavian Petrus, ALI CUZA University, ROMANIA
Prof. M.A. Hellberg, University of Natal, SO AFRICA
Dr. Johan de Villiers, Plasma Physics, Nucor, SO AFRICA
Fusion Div. Library, JEN, SPAIN
Prof. Hans Wilhelmson, Chalmers Univ Tech, SWEDEN
Dr. Lennart Stenflo, University of UMEA, SWEDEN
Library, Royal Inst Tech, SWEDEN
Centre de Recherchesen, Ecole Polytech Fed, SWITZERLAND
Dr. V.T. Tolok, Kharkov Phys Tech Ins, USSR
Dr. D.D. Ryutov, Siberian Acad Sci, USSR
Dr. G.A. Eliseev, Kurchatov Institute, USSR
Dr. V.A. Glukhikh, Inst Electro-Physical, USSR
Institute Gen. Physics, USSR
Prof. T.J.M. Boyd, Univ College N Wales, WALES
Dr. K. Schindler, Ruhr Universitat, W. GERMANY
Nuclear Res Estab, Julich Ltd, W. GERMANY
Librarian, Max-Planck Institut, W. GERMANY
Bibliothek, Inst Plasmaforschung, W. GERMANY
Prof. R.K. Janev, Inst Phys, YUGOSLAVIA